PILOT STUDY OF GENERAL PREDICTIVE CONTROL + INTEGRAL COMPENSATOR FOR POWERED PROSTHETIC LEGS

Ricardo Bautista-Quintero[1,2], Rickey Dubay[1], Juan A. Carretero[1] and Miguel A. Díaz-Rodríguez[3]
[1] *Department of Mechanical Engineering, University of New Brunswick, Fredericton, NB, Canada*
[2] *Departamento de Metal Mecánica, Instituto Tecnológico de Culiacán, Sinaloa, México*
[3] *Departamento de Tecnología y Diseño, Facultad de Ingeniería, Universidad de los Andes, Mérida, Venezuela*
Email: r.bautista@unb.ca

ABSTRACT

In the last decade, technology related to powered prosthetic legs has demonstrated solid potential towards returning fully functional capabilities to millions of lower-limb-amputees. The remarkable advantages in such prosthetic legs have integrated state-of-the-art mechatronic systems which are able to read bio-electric-signals and convert them into mechanical human-like leg movements. However, replicating the inherent complexity of human mobility is not a trivial control problem. In fact, the strategies for this application must be capable to control prosthetic actuators efficiently (optimising energy consumption) and be clinically reliable ensuring stability. In this context, the paper introduces a control approach based on General Predictive Control (GPC) + Integral compensator. This technique is based on a prediction mechanism that optimally minimizes the sum of the square errors between the future prediction and current measurements. Although robustness of the optimal GPC has been widely evaluated for linear systems, this approach uses a non-linear model of a Two-Degrees-of-Freedom prosthetic leg. A model identification algorithm estimates the transfemoral device dynamic behaviour in order to design a GPC control partially decoupled in two decentralized subsystems. An integral compensator is added to reduce the uncertainties due to residual dynamics caused by link interaction and friction torques in the joints.

Keywords: Power Prosthetic Leg; GPC+Integral Approach; System Identification, Non-Linear Model, Mechatronic system.

1. INTRODUCTION

Limb loss has represented one the most complex problem faced by humanity throughout history. In order to mitigate it, prosthetic limbs emerged about 3500 years ago [1]. However, even today, the social, psychological and economic impact is still not well addressed. For instance, the quality of life of lower-limb amputees is dramatically reduced since secondary pathological issues are presented such as osteoarthritis, back pain, and depression [2]. The latest technology of such devices are still far from being available, most particularly, for people living in undeveloped countries. Most of the available technology is based on passive devices. For lower-limbs amputees prosthetic legs have been the only choice due to the lack of technological maturity of active (*e.g.*, motorized) prosthetic devices. Unfortunately, even today, people who wear the most advanced passive prosthetic limbs still find difficulty to walk on slopes, climb stairs or uneven terrains, since the non-symmetrical gait increases the muscular effort either on residual limbs [3]. The new generation of active prosthetic devices improves mobility in general [4]. Particularly, motorized prosthetic legs represent the ultimate technological goal that might be able to mimic the gait of an intact person. In this context, the hypothesis of this pilot study states the following: there must be a synergistic combination of three fundamental tools that can be efficiently used to design cost-effective prosthetic devices that are energy-efficient and clinically viable. These tools are 1) Bionic know-how that interfaces the biological tissue with a mechatronic system, 2) Portable high-efficiency torque actuators and 3) Understanding of the vast theoretical knowledge related to automatic control of biped robots. These key technological and theoretical components have been recently available, and the ultimate goal of this project is meant to find this synergistic combination of them that could result in a prosthesis design with human-like capabilities.

1.1. Control Design Challenges of Motorized Prosthetic Legs

Technology related to motorized prosthetic legs has reached a level of maturity that might significantly improve mobility of lower limb amputees patients around the world. However, there are some important challenges in the field of automatic control due to be solved. In order to understand such challenges, a brief introduction in this matter is presented as follows. The history of prosthetic devices started with rigid passive legs (*i.e.*, no actuators) and they have been the only choice for those who has suffered a leg loss [5]. Flexible and more complex passive devices (*i.e.*, artificial limbs) slowly emerged in the last decades [3] in order to improve adaptability and locomotion. These artificial limbs are usually customized for every single patient. More metabolic energy effort, less stability and slow movements than able-body locomotion is reported [6].

On the other hand, powered prosthetic legs could potentially recover all function of lower-limb amputees [5]. The gait cycle of these prosthetic legs is determined based on different "time periods", better known as gait-cycles. Each gait-cycle has its own control model [7]. Dealing with the transition between these multiple cycles is a complex matter that mainly depends on the feedback sensors of the prosthetic device [8]. Each control model requires the simultaneous modification of parameters such as torque, speed, and desired impedance at the contact point [6]. A highly reliable estimation in the gait cycle, along with the control tuning gains for every single patient, is still an open problem [4]. The current research in this area has partially solved the problem reducing it to the minimum necessary cycles and tuning the control parameters by an expert [6].

Reduction in the gait cycles increases the system reliability, however this reduces the mobility. The hand-tuned procedures are not a practical option for a large number of patients, since it requires long periods of testing.

1.2. Control prosthetic lower limbs inspired by Biped Robot strategies

Control theory has been formulated by researchers over the last centuries with rigorous mathematical support for a wide diversity of problems. Particularly, literature on control of motorized prosthetic limbs is a new application area with numerous challenges related to robustness, stability, and adaptability. Among many strategies Proportional Integral Derivative (PID) control has been, by far, extensively used in many applications related to rehabilitation, among others [4]. The core of this technique provides a control signal based on an error (*e.g.*, the difference between set-point(s) and output signal(s)). The regulatory effect of PID is able to ensure control stability for many under estimate dynamic systems [9]. However, recent applications of such technique applied to legged robots have shown unstable behaviour when high robustness is required [7]. One common strategy to overcome such problem deals with the inclusion on the dynamic model a desired impedance (*e.g.*, join stiffness or viscosity) caused by the contact point on the ground. Most of the PID family (*e.g.*, PD, PD+G, PI, *etc.*) in combination with other strategies were evaluated in motorized prosthetic prototypes, these approaches were implemented on biped locomotion algorithms. Some of these implementations use heuristic approaches which provide the fine tuning of the controller gains, for instance: Genetic Algorithms in [10] were used to optimize the gait sequences by tuning the gains in order to reduce the energy consumption. Unfortunately, the high computational burden of such algorithm is impractical for portable embedded systems [11]. Another common heuristic approach based on Artificial Neural Networks (ANN) which is based on a learning basis. In this context, one of the most common control strategies based on ANN used for biped robots is Back-propagation algorithm [12]. The main limitation is the memory and processing time required to train in real-time the complex dynamic bipedal locomotion is still an undergoing research [4]. Most of the established control approaches used in bipedal locomotion are based on quasi-static models which can reduce mobility when they are required to implement in a motorized prosthetic devices [5]. Non-linear dynamic models have been used to evaluate by simulation different system control algorithms for biped robots. Similarly prosthetic are commonly modelled as full-biped models in order to consider the intricate dynamic interaction between the legs and the links (*e.g.*, [7]). One of the common control algorithms used for these non-linear models is the Sliding Mode Control (SMC) which is a powerful approach for applications modelled as non-linear plants [13]. The variable structure of such control allows controlling biped robots in different phases; the stability is guarantee when a Lyapunov candidate function is chosen properly. Nevertheless, some experimental work in this field uses the criteria of Zero Moment Point (ZMP) for modelling the upper body which may allow stability under very low speed ranges (*e.g.*, [7]) that limits the use of SMC for such application. Also, Partial Feedback linearization approach has been a successful technique that maintains the system stable when the dynamic model is fully determined [6]. Unfortunately, model uncertainties and structural variations can guarantee stability, so that, in practice a PD compensator is commonly added to compensate the remaining dynamics not considered in the model. Other control techniques have been used in prosthetic lower limb applications inspired from biped robot designs. However, these techniques are out of the scope of this literature review. A summary of the specific challenges to control a prosthetic device of a one leg amputee system of 2 degrees-of-freedom (DOF) is presented in [4]. These challenges are specifically related to find a control design that can reliable enough to switch among phases. Also the fine tuning algorithm can be a systematic process for different patients, tasks and time-variant conditions [6].

Particularly, the problem described in this study is related to the design of a robust adaptive control technique for a lower-limb prosthetic device capable of tracking the human-gait trajectories, in order to co-ordinate a walking sequence with the intact leg. In this context, the paper introduces a control approach General Predictive Control (GPC) + Integral compensator which can not only be adaptive but also computationally inexpensive. This technique includes a prediction mechanism that optimally minimizes the sum of the square errors between the future prediction and current measurements. Although robustness of the optimal GPC has been widely evaluated for linear systems, this approach is based on a non-linear model of a 2 DOF prosthetic leg. A model identification algorithm is used to estimate the transfemoral device dynamic behaviour in order to design a GPC control partially decoupled in two decentralized subsystems. Here, an integral compensator is meant to reduce the uncertainties due to residual dynamic caused for both links interaction and friction torques in the joints.

The paper is organized as follows, Section 2 deals with two stages for obtaining the dynamic model of the prosthesis device using a non-linear MIMO plant and reduced to a couple of SISO linear models. Section 3 describes how to design the control based on GPC+I for the linearized plant obtained in the previous section. Results are described in Section 4 and the following section provides conclusions to this paper.

2. MODEL IDENTIFICATION OF A 2-DOF LOWER PROSTHETIC LIMB

This section describes the dynamic system used to describe the mathematical behaviour of a 2-DOF serial mechanism. This model represents a simplified model of both the remaining leg and the prosthetic limb, however real parameters of this model are not easy to calculate. In fact, the fusion of a serial mechanism along with biological tissue contains lumped parameters that are not fully understood. Instead of trying to calculate these parameters, the proposed approach uses a standard regression model based on a least square method to estimate time-invariant parameters. The proposed identification algorithm is divided in two stages: 1) Identification of Multiple-Input and Multiple-Output (MIMO) dynamic model of 2-DOF serial mechanism that considered lumped parameters (biological + mechanical) and 2) identification of a Single-Input Single-Output (SISO) dynamic model for control purposes. The first identification stage provides the numerical information of the full leg in order to identify (second stage) each joint independently for control purposes. A general diagram of the prosthetic leg is shown in the Fig. 1.

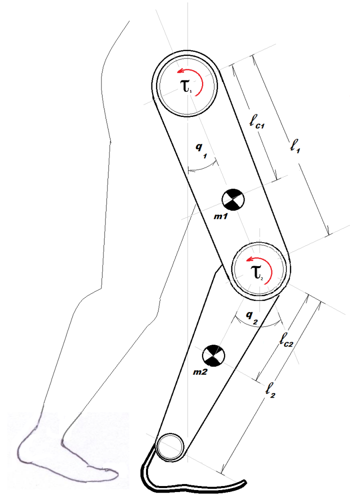

Fig. 1. Prosthetic leg configuration based on 2-DOF serial mechanism.

2.1. First stage of the Model Identification

Model system identification was originally proposed by mathematicians whose historically tried to make system models based on statistics, regression techniques, and many other tools. This technique establishes a model constructed by means of an appropriate input/output map where the dynamic structure of the system is either full known or partially known. The input/output map for this application is defined in linear in parameters in order to use a standard regressor. This regressor provides the parameters of the system such as inertia moments, lengths of the limbs where the centre of mass is located, *etc*. Although the algorithm is valid for time-invariant cases, in practice, this algorithm should identify a new set of parameters every time the system changes. Online identification of such parameters provides adaptability if a control strategy is combined along with this identification technique.

Based on Fig. 1, a dynamic model can be obtained by finding the energy-model of the system. The so called Lagrange formulation (see details in [14]) is used to obtain the dynamic structure of the prosthetic leg which is modelled as a 2-DOF serial link mechanism as:

$$\mathbf{M}(\mathbf{q})\ddot{q}+\mathbf{C}(\mathbf{q},\dot{\mathbf{q}})\dot{q}+\mathbf{g}(\mathbf{q})+\mathbf{f}(\dot{\mathbf{q}})=\tau \tag{1}$$

where: q is a 2×1 angular position vector, $\dot{q}$ is a 2×1 angular velocity vector, $\ddot{q}$ is a 2×1 angular acceleration vector. $M(q)$ is a 2×2 inertia matrix whose components are described as:

$$\mathbf{M}(\mathbf{q})=\begin{bmatrix} m_1l_{c1}^2+m_2(l_1^2+l_{c2}^2+2l_1l_{c2}\cos(q_2)+I_1+I_2) & m_2(l_{c2}^2+l_1l_{c2}\cos(q_2)+I_2) \\ m_2(l_{c2}^2+l_1l_{c2}\cos(q_2)+I_2) & m_2l_{c2}^2+I_2 \end{bmatrix} \tag{2}$$

$C(q,\dot{q})$ is a 2×2 Coriolis matrix term:

$$\mathbf{C}(\mathbf{q},\dot{\mathbf{q}})=\begin{bmatrix} -m_2l_1l_{c2}\sin(q_2)\dot{q}_2^2 & -m_2l_1l_{c2}\sin(q_2)(\dot{q}_1+\dot{q}_2) \\ m_2l_1l_{c2}\sin(q_2)\dot{q}_1 & 0 \end{bmatrix} \tag{3}$$

$g(q)$ is a 2×1 gravity vector:

$$\mathbf{g}(\mathbf{q})=\begin{bmatrix} m_1l_{c2}+m_2l_1g\sin(q_1)+m_2l_{c2}\sin(q_1+q_2)) \\ m_2l_{c2}g\sin(q_1+q_2) \end{bmatrix} \tag{4}$$

and $f(\dot{q})$ is a 2×1 vector that represents both Coulomb and viscous friction torques:

$$\mathbf{f}(\dot{\mathbf{q}}) = \begin{bmatrix} b_1\dot{q}_1 + f_{c_1} sgn(\dot{q}_1) \\ b_2\dot{q}_2 + f_{c_2} sgn(\dot{q}_2) \end{bmatrix} \tag{5}$$

Since the system in Equation (1) is linear in parameters, the model can be re-written as a function that depends of positions and their derivatives. That is:

$$\mathbf{M}(\mathbf{q})\ddot{q} + \mathbf{C}(\mathbf{q},\dot{\mathbf{q}})\dot{q} + \mathbf{g}(\mathbf{q}) + \mathbf{f}(\dot{\mathbf{q}}) = \mathbf{Y}(q,\dot{q},\ddot{q})\Phi = \tau \tag{6}$$

where $\Phi = [\phi_1, \phi_2, \phi_3, \phi_4, \phi_5, \phi_6, \phi_7, \phi_8, \phi_9]^T$ can be defined by:

$$\Phi = \begin{bmatrix} m_1 l_{c1}^2 + m_2 l_1^2 + m_2 l_{c2}^2 + I_1 + I_2 \\ l_1 m_2 l_{c2} \\ m_2 l_{c2}^2 + I_2 \\ g(l_{c1} m_1 + m_2 l_1) \\ g m_2 l_{c2} \\ b_1 \\ b_2 \\ f_{c1} \\ f_{c2} \end{bmatrix} \tag{7}$$

Based on Equation (1) and the lumped parameters proposed in Equation (7), $\mathbf{Y}(q,\dot{q},\ddot{q})$ corresponds to Equation (8) which is a 2×9 matrix:

$$\mathbf{Y}(q,\dot{q},\ddot{q}) = \begin{bmatrix} \ddot{q}_1 & 3\ddot{q}_1\cos(q_2) + \dot{q}_1\sin(q_2)(\dot{q}_1 - 2\dot{q}_2) & \ddot{q}_1 & \sin(q_1) & \sin(q_1+q_2) & \dot{q}_1 & 0 & sgn(\dot{q}_1) & 0 \\ 0 & \dot{q}_2\cos(q_2) - \sin(q_2)\dot{q}_2^2 & 2\ddot{q}_2 & 0 & \sin(q_1+q_2) & 0 & \dot{q}_2 & 0 & sgn(\dot{q}_2) \end{bmatrix} \tag{8}$$

The identification system is evaluated using values similar to those in [15] (see Table 1a).

An estimation of Φ can be called $\hat{\Phi}$ and it is calculated based on Least Mean Squares (LMS) algorithm. Minimization of the LMS difference between the parameters Φ (obtained experimentally by the output signals in matrix Y) and the estimation of the model. A partial derivative of the LMS with respect the parameters Φ equalized to zero gives the parameter estimated from Equation (9).

$$\hat{\Phi} = (\mathbf{Y}_i^T\mathbf{Y}_i + \lambda I)^{-1}\mathbf{Y}_i\tau_i \tag{9}$$

where $\mathbf{I}$ is the identity matrix, λ is a constant regularization parameter (when $\mathbf{Y}_i^T\mathbf{Y}_i$ is ill-conditioned), $i = 1...N_S$ (with N_S being the number of the samples, N_S = SimulationTime/SampleTime and $\mathbf{Y}_i$ is $2i \times 9$ and τ_i is $2i \times 1$.

The system can be described with the following model based on vector Φ:

$$\hat{\mathbf{M}}(\mathbf{q}) = \begin{bmatrix} \phi_1 + 2\phi_2\cos(q_2) & \phi 3 + \phi 2\cos(q_2) \\ \phi_3 + \phi_2\cos(q_2) & \phi_3 \end{bmatrix} \tag{10}$$

$$\hat{\mathbf{C}}(\mathbf{q},\dot{\mathbf{q}}) = \begin{bmatrix} -2\phi_2\sin(q_2)\dot{q}_2 & -\phi_2\sin(q_2)\dot{q}_2) \\ \phi_2\sin(q_2)\dot{q}_1 & 0 \end{bmatrix} \tag{11}$$

$$\hat{\mathbf{g}}(\mathbf{q}) = \begin{bmatrix} \phi_4\sin(q_1) + \phi_5\sin(q_1+q_2) \\ \phi_5\sin(q_1+q_2) \end{bmatrix} \tag{12}$$

$$\hat{\mathbf{f}}(\dot{\mathbf{q}}) = \begin{bmatrix} \phi_6\dot{q}_1 + \phi_8 sgn(\dot{q}_1) \\ \phi_7\dot{q}_2 + \phi_9 sgn(\dot{q}_2) \end{bmatrix} \tag{13}$$

Parameter	Simbol	Value	*Units*
Length link 1	l_1	0.40	m
Mass link 1	m_1	6	kg
Mass link 2	m_2	3.5	kg
CoM Link 1	l_{c1}	0.091	m
CoM Link 2	l_{c2}	0.048	m
Inertia Link 1	I_1	0.5	$kg\ m^2$
Inertia Link 2	I_2	0.1	$kg\ m^2$
Viscous coeff. 1	b_1	0.6	$N\ m\ s$
Viscous coeff. 2	b_2	0.25	$N\ m\ s$
Coulomb coeff. 1	f_{c1}	1	$N\ m$
Coulomb coeff. 2	f_{c2}	0.75	$N\ m$
Gravity	g	9.81	m/s^2

(a) Real values suggested

Parameter	Symbol	*Units*
Mass of link	m	kg
Mass of link (CoM)	m_b	kg
Length of the link	l	m
Arm's moment of inertia	J	$kg\ m^2$
Motor's moment of inertia	J_M	$kg\ m^2$
Inertia centre gravity	J_L	$kg\ m^2$
Friction coeff. joint	f_L	$N\ m\ s$
Friction coeff. motor	f_M	$N\ m\ s$
Motor constants	K_a	$N\ m\ Ohms/V$
	K_b	s/rad
	R_a	$Ohms$
Gear Box ratio	r	$dimensionless$

(b) Parameters for each link of the mechanism

Table 1. Dynamic parameters.

2.2. Second stage of the Model Identification

The second part of the model identification algorithm is designed to find the parameters of each link independently based on the MIMO dynamic system presented previously. The model of each link (1,2) can be theoretically as:

$$(J+ml^2)\ddot{q}+f_L\dot{q}+(m_bl_b+ml)g\sin(q)=\tau_{(1,2)} \tag{14}$$

In practice, and based on Euler-Lagrange equation [14], the complete dynamic model of each link combines the expression given by Equation (14) and the internal dynamic model of the DC servomotor (*i.e.*, the actuator for each link), and the gear-box. Each link + actuator dynamic model is presented in the following equation and its parameters (symbols and units can be seen in Table 2):

$$\left(J_m+\frac{J_L}{r^2}\right)\ddot{q}+\left(f_m+\frac{f_L}{r^2}+\frac{K_aK_b}{R_a}\right)\dot{q}+\frac{k_L}{r^2}\sin(q)=\frac{K_a}{rR_a}v_{(1,2)} \tag{15}$$

where: $k_l=g(m_bl_b+ml)$

Equation (15) can be re-written as a linear map between the input voltage and the output $\mathbf{Y}_{(1,2)}$ as follows:

$$\left(J_m+\frac{J_L}{r^2}\right)\ddot{q}+\left(f_m+\frac{f_L}{r^2}+\frac{K_aK_b}{R_a}\right)\dot{q}+\frac{k_L}{r^2}\sin(q)=\mathbf{Y}_{(1,2)}(q,\dot{q},\ddot{q})\Phi_{1,2}=\frac{K_a}{rR_a}v_{(1,2)} \tag{16}$$

where (1,2) stands for link 1 and link 2, $\Phi_{(1,2)}=[\phi_a,\phi_b,\phi_c]^T$ can be defined by:

$$\Phi_{(1,2)}=\begin{bmatrix} J_m+\frac{J_L}{r^2} \\ f_m+\frac{f_L}{r^2}+\frac{K_aK_b}{R_a} \\ \frac{k_L}{r^2} \end{bmatrix} \tag{17}$$

and $\mathbf{Y}_{(1,2)}(q,\dot{q},\ddot{q})$ is written based on Equation (15), so that $Y_{1,2}$ is proposed as follows:

$$Y_{(1,2)}(q,\dot{q},\ddot{q})=\left[\sin(q)\ \dot{q}\ \ddot{q}\right] \tag{18}$$

Since the regressor in Equation (18) is still a non-linear model, it can be assumed that $\sin(q)\approx q$ when $q\approx 0$, then the GPC control system can be designed, around this equilibrium point, as a linear system. A simplified diagram of the two stages of the system identification can be seen in Figure 2.

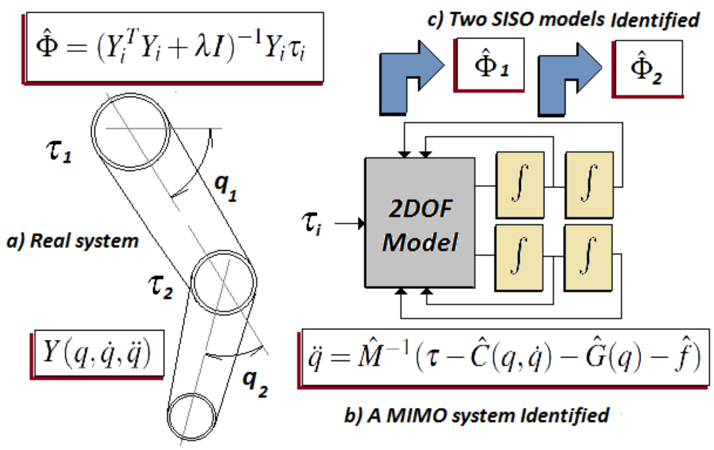

Fig. 2. Two model-identification stages for the prosthetic dynamic device. Based on real data, a 2-DOF dynamic model is constructed. Based on this numerical data, two SISO systems represent the dynamics of each joint with reciprocal interaction between the two.

3. CONTROL DESIGN BASED ON A GPC+I

A generalised predictive control was first presented in [16]. This type of control integrates some of the common ideas of previous MPC control algorithms (see a survey of these previous approaches [17]). GPC has been is widely accepted in both academia and industry since it can cope with unstable open-loop plants and minimum phase features [18]. The GPC algorithm is based on obtaining a sequence of future control signals in a fashion to minimise a multi-stage cost function defined over a prediction horizon. The predictions should be generated accurately and based on a real dynamic system in order to supply a proper output signal.

The features of GPC control have been combined with adaptive algorithms which are meant to provide an accurate discrete model either off-line or on-line execution [19]. Description and implementation of different adaptive predictive control is been explored [20]. In addition, cascade configurations have also been proposed, see the survey in [21]. While adaptive techniques may lead to fragility in the implementation [11], cascade counterparts are not easily capable of coping with structural uncertainties. To this end, the optimization capability combined with the simple and adaptive features make GPC a practical choice suggested in this paper for this prosthetic system device.

Since the MIMO Dynamic model has been divided into a couple of SISO plants, the GPC strategy represents the system with an accurate CARIMA model (see details in [16] and [18]). This representation of a SISO linear plant in z-transform is based on the discrete model of a transfer function:

$$A(z^{-1})y(t) = z^{-d}B(z^{-1})u(t-1) + C(z^{-1})e(t) \tag{19}$$

where $e(t)$ is the white noise and

$$\begin{aligned} A(z^{-1}) &= 1 + a_1 z^{-1} + a_2 z^{-2} + \ldots + a_{na} z^{-na} \\ B(z^{-1}) &= b_0 + b_1 z^{-1} + b_2 z^{-2} + \ldots + b_{nb} z^{-nb} \\ C(z^{-1}) &= 1 + c_1 z^{-1} + c_2 z^{-2} + \ldots + c_{nc} z^{-nc} \end{aligned} \tag{20}$$

where d is the dead time of the system.

From the functions presented in Equation (20), a so called CARIMA model can be written as follows:

$$A(z^{-1})y(t) = B(z^{-1})z^{-d}u(t-1) + C(z^{-1})\frac{e(t)}{\Delta} \tag{21}$$

The GPC is meant to apply a control sequence in order to minimise the multi-stage cost function of the form:

$$J(N_1,N_2,N_u) = \sum_{j=N_1}^{N_2} \delta(j)[\hat{y}(t+j|t)] - w(t+j)]^2 + \sum_{j=1}^{N_u} \lambda(j)[\Delta u(t+j-1)]^2 \tag{22}$$

where: $\hat{y}(t+j|t)$ is an optimum j-step ahead prediction of the system output data up to the time t, N_1 and N_2 are the minimum and maximum costing horizons, N_u is the control horizon, $\delta(j)$ and $\lambda(j)$ are the weighting sequences and $w(t+j)$ is the set-point. The main goal of GPC is computing the output signal $u(t), u(t+1), \ldots u(t+\Delta t)$ in order the controlled variable $y(t+j)$ follow the set-point by minimizing the cost function J. The solution to this minimization problem starts by using Diophantine equation:

$$1 = E_j(z^{-1})\tilde{A}(z^{-1}) + z^{-j}F_j(z^{-1}) \tag{23}$$

where:

$\tilde{A} = (1-z^{-1})A(z^{-1})$,
$F_1(z^{-1}) = z[1-\tilde{A}(z^{-1})]$,
$G_{j+1} = E_{j+1}B(z^{-1})$,
$E_j(z^{-1}) = e_{j,0} + e_{j,1}z^{-1} + \ldots + e_{j,j-1}z^{-(j-1)}$
$E_1 = 1$, $E_{j+1} = E_j + f_{j,0}z^{-j}$,
$F_{j+1}(z^{-1}) = z[F_j - f_{j,0}\tilde{A}(z^{-1})]$,
$F_j(z^{-1}) = f_{j,0} + f_{j,1}z^{-1} + \ldots + f_{j,na}z^{-na}$,

Based on the previous polynomials, two expressions are calculated 1) prediction and 2) free-response of the system; the dynamic matrix $\mathbf{G}$ made up of n_u columns of the coefficients of polynomial $G_j(z^{-1})$ the shifted one single row, and P is the prediction horizon. This is similar to the procedure followed in dynamic matrix control designs [18]. The coefficients of $G_j(z^{-1})$ are: $g_1, g_2, g_3, \ldots, g_{N_2}$.

According to [16], $N_2\Delta t$ can be chosen as large as the rise time of the system, that implies that the N_2 determines the length of the prediction $\hat{y}$. N_1 must be larger that $d+1$.

The free response of each link is calculated based on the following equation:

$$f_{j+1} = z\left[1-\tilde{A}(z^{-1})\right] f_j + B(z^{-1})\Delta u(t-d+j) \tag{24}$$

and $f_0 = y(t)$ and $\Delta u(t+j) = 0$ for $j \geq 0$.

The minimization of the cost function J in the case of white noise added and no constraints of the control signals leads to find the control signal u which is the optimal prediction according to the features previously described (see details in [16]). This is given by the following expression:

$$u = (\mathbf{G}^T\mathbf{G} + \lambda\mathbf{I})^{-1}\mathbf{G}^T(SP - f_R) \tag{25}$$

The control signal depends only on the first row of the matrix $(\mathbf{G}^T\mathbf{G} + \lambda\mathbf{I})^{-1}\mathbf{G}^T$ which can be classified as a gain term K in standard nomenclature [18], so that the control u is given by:

$$\Delta u = K(SP - f_R) \tag{26}$$

with:

$$\begin{aligned} K &= k_1 + k_2 + \ldots + k_{N2} \\ \Delta u_2(t) &= (1-z^{-1})u_2 \\ \Delta u_2(t) &= u_2(t) - u_2(t-1) \\ \Delta u_2(t-1) &= u_2(t-1) - u_2(t-2) \end{aligned} \tag{27}$$

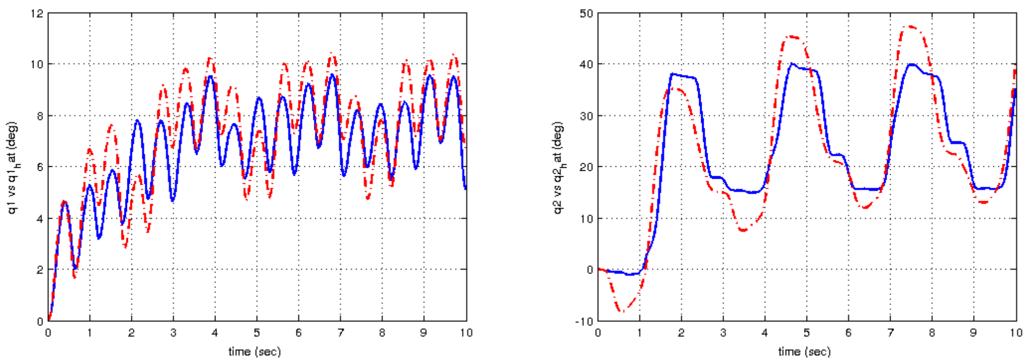

Fig. 3. First stage of the system identification (MIMO model) original system (solid-blue) response *vs.* Identified plant (dashed-red).

The free response (f_R) in matrix form is:

$$f_R = \begin{bmatrix} g_{(1,n_b+1)}\Delta u_{t-1} & f_{1,0}y_t & f_{1,1}z^{-1}y_{t-1}\dots & f_{1,n_a}z^{-n_a}y_{t-n_a} \\ g_{(2,n_b+1)}\Delta u_{t-1} & f_{2,0}y_t & f_{2,1}z^{-1}y_{t-1}\dots & f_{2,n_a}z^{-n_a}y_{t-n_a} \\ \vdots & \vdots & \vdots & \vdots \\ g_{(N_2,n_b+1)}\Delta u_{t-1} & f_{N_2,0}y_t & f_{N_2,1}z^{-1}y_{t-1}\dots & f_{N_2,n_a}z^{-n_a}y_{t-n_a} \end{bmatrix} \tag{28}$$

Rearranging all equations to implement the control signal u yields:

$$u = -K(f_R) + u(t-1) - k_1 u(t-2) + K(SP); \tag{29}$$

where $SP = [sp(t+1), sp(t+2), ..., sp(t+N_2)]^T$. The coefficients of the $\mathbf{G}$ matrix are calculated recursively form given in the following algorithm, based on [16]. Note that, the discrete model is now based on a second order system since the integral term was included, the relation between the input (voltage) and output (angular position).

4. RESULTS

This section shows some details of the experimental simulation of the model and the control results. The first stage of the identification collects the input-output map between the numerical values of the matrix Equations (8) and the vector τ which is the excitation signal given by the following expression:

$$\tau_1 = 3.53[(1-\exp^{-0.8t}) + \sin(10.8t) + 0.5\sin(24.6t) + 0.25\sin(43.2t) \tag{30}$$

$$\tau_2 = 0.81[(1-\exp^{-0.8t}) + \cos(2.2t) + 0.405\cos(4.44t) + 0.201\cos(8.88t) \tag{31}$$

Equations (30) and (31) are signals that improve the conditioning of the identification matrix, these values were similar to values chosen in [15]. Figure 3 shows the response of the identified model and the original system, as can be seen the identified model is able to follow closely the original system. The excitation signal still requires some adjustment in order to track more accurately the original signal, particularly for q_2.

The following values were obtained by the numerical simulation, shown in Table 2.

The second stage of the system identification algorithm is meant to predict the dynamic of each join independently. The values obtained are $\hat{\Phi}_1 = [1.103, 1.79, 20.89]$ and $\hat{\Phi}_2 = [0.0613, 0.3980, 1.6677]$ see

Lumped Parameter	Real value	Identified value
ϕ_1	1.2178	1.2217
ϕ_2	0.0672	0.0623
ϕ_3	0.1081	0.0296
ϕ_4	19.0903	18.4988
ϕ_5	1.6481	1.5420
ϕ_6	0.6	0.9072
ϕ_7	0.25	0.686
ϕ_8	1.0	1.0885
ϕ_9	0.75	0.75

Table 2. Comparison real values *vs.* identified values

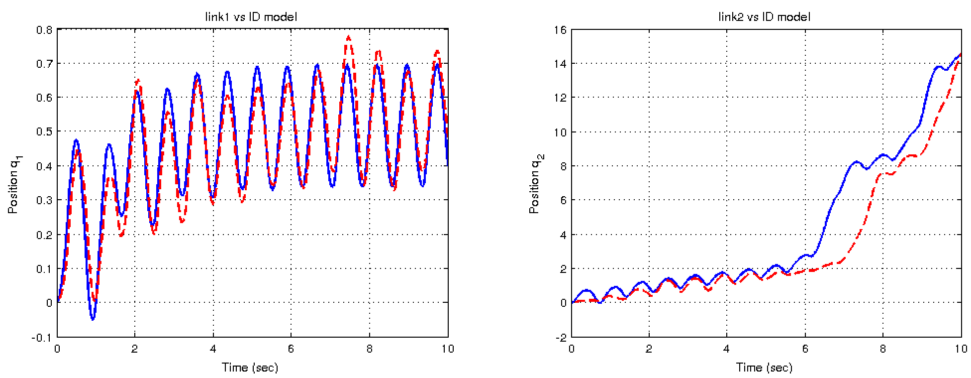

Fig. 4. Second stage of the system identification (numerical values of the general dynamic plant) (solid-blue) response *vs.* identified plant (dashed-red).

Figure 4. Based on these parameters two SISO systems are defined to design the GPC control approach of the following section.

The control signals u_1 and u_2 are obtained by Equation (29) and the parameters for the upper link are: $\lambda_1 = 0.0001$, the prediction horizon is $P_1 = 22$, and the control horizon $n_u = 2$. For the lower link are: $\lambda_2 = 0.041$, the prediction horizon is $P_2 = 17$, and the control horizon $n_u = 2$. The control structure and plant is shown in Figure 5. The integral compensator is meant to reduce the steady-state error caused for static forces not considered in the control model design. The gains for this compensator are obtained after a few iterations.

A human gait reference signal is used to evaluate performance of the control strategy and it is compared with a reference controller in order to show the efficient o the GPC+I in terms of position tracking, see Figure 6.

The gains used for the GPC+I controller are:
K_{GPC1}=$[-8866.57, 15790.30, -7117.22, -0.6758, -0.3241]$ (upper limb)
K_{GPC2}=$[-505.24, 877.01, -386.77, -0.677, -0.32]$ (lower limb).
Similarly the system is compared with a set of PID independent joint controllers, the compensator formula of this PID is $K_P + K_I T_s(\frac{1}{z-1}) + K_D \frac{N}{1+NT_s(\frac{1}{z-1})}$ which gains are: $K_P = 200$, $K_D = 5$, $K_I = 2$ and $N = 50$ (for the upper limb joint) $K_P = 50$, $K_D = 1$, $K_I = 2$ and $N = 50$ (for the lower limb joint).

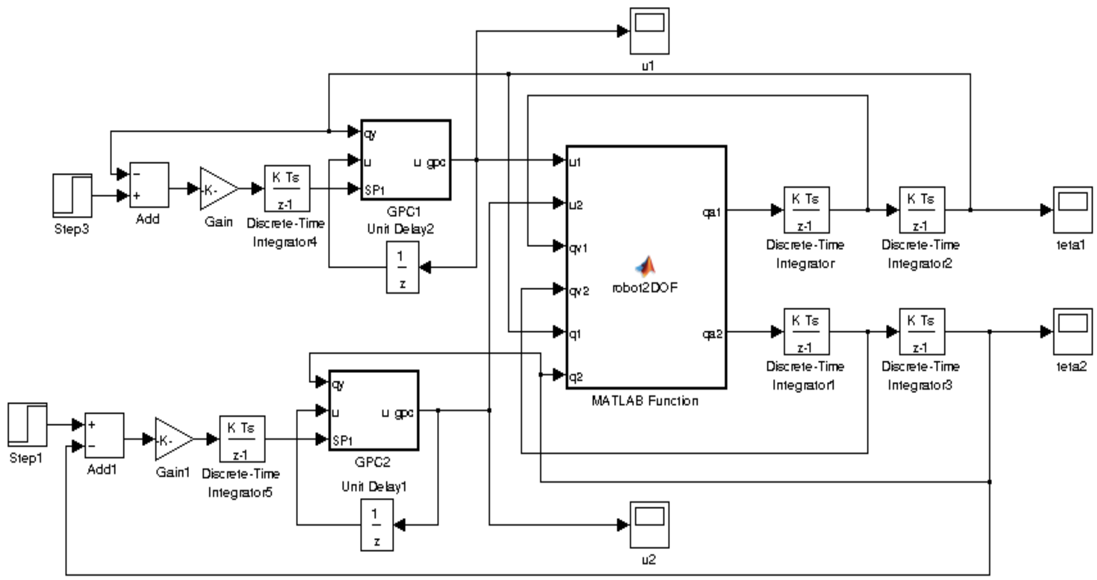

Fig. 5. Block diagram of the digital control system GPC+Integral compensator applied to the nonlinear MIMO plant.

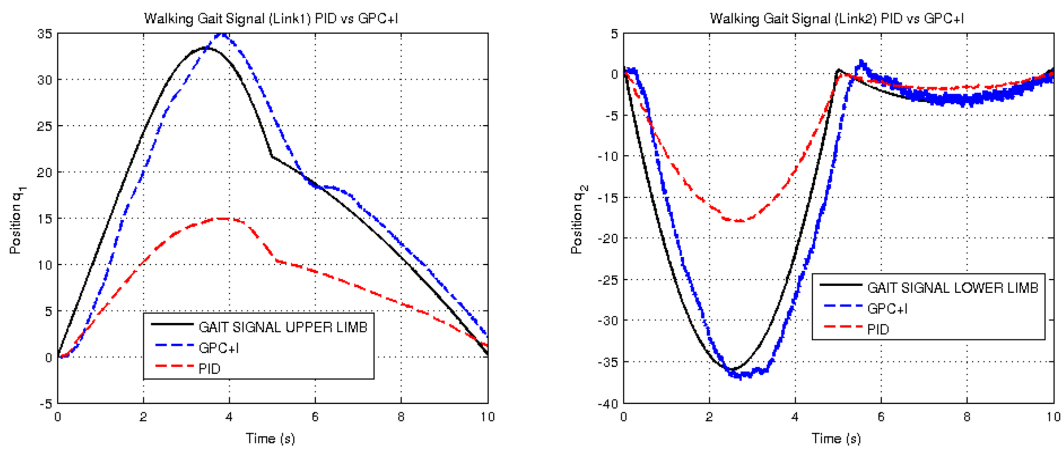

Fig. 6. Tracking gait trajectories of a lower prosthetic device, a comparison response between GPC and PID control

5. CONCLUSIONS

The main focus of the paper was a pilot study of a predictive control strategy used for prosthetic motorized artificial limbs. Due to the complexity of the different stages in the human gait tasks (*e.g.*, walking, standing, stair climbing) an advance adaptive and robust control technique is the possible future solution. The proposed controller and the evaluation performance of this paper introduces a combination of model identification techniques, General Predictive Control + Integral compensator for a decoupled dynamic model. The rationale of using an advance control technique comes from biped robot techniques which are closely compatible with the control requirements of power limb prosthetic devices. The main result of this pilot study can conclude that GPC+I is a simple controller to be implemented since only a few gains are needed to generate the control law. The performance of GPC for this simple experiment performs better tracking gait trajectory in comparison with PID controller. However, further experiments and real-time experiments may lead to more important conclusions. The GPC control strategy can be adaptive in order to auto tuning the system for every single patient, that may reduce the time to adjust the control features. A full dynamic model was used to verify the performance of two separate GPC join controller and the robustness of this approach was particularly efficient. This method can be potentially implemented in a real prosthetic device since the optimal features of the GPC can be exploited in order to reduce the energy required to move the limb for cost-effective applications. Additionally, another degree of freedom can be added to the system in order to have an ankle powered by a third actuator, so far it was considered a passive component.

ACKNOWLEDGEMENTS

The authors acknowledge the financial support from the Natural Science and Engineering Research Council of Canada (NSERC), FONACIT Venezuela, CONACYT scholarship 326912/381134 and also the SNI-México.

REFERENCES

1. David, R. *Egyptian Mummies and Modern Science*. Cambridge University Press, 2008.
2. Pell, J.P., Donnan, P.T., Fowkers, F.G. and Ruckler, C.V. "Quality of life following lower limb amputation for peripherical arterial disease." *Eur. J. Vasc. Surg.*, Vol. 7, No. 4, pp. 448–451, 1993.
3. Seroussi, J.P. and Gitter, A. "Mechanical work adaptations of above-knee amputee ambulation." *Arch. Phys Med. Rehab*, Vol. 77, pp. 1209–1214, 1996.
4. Samad, T. and Annaswamy, A. "The impact of control technology." *IEEE, Control Systems Society*, Vol. 2, pp. 27–28, 2014.
5. Johansson, J., Sherrill, D., Riley, P., Bonato, P. and Herr, H. "A clinical comparison of variabledamping and mechanically passive prosthetic knee devices." *American Journal of Physical Medicine & Rehabilitation*, 2005.
6. Gregg, R., Lenzi, T., Hargrove, L. and Sensinger, J. "Virtual constraint control of a powered prosthetic leg: From simulation to experiments with transfemoral amputees." *Robotics, IEEE Transactions on*, Vol. 30, No. 6, pp. 1455–1471, Dec 2014.
7. Nakanishi, J., Morimoto, J., Endo, G., Cheng, G., Schaal, S. and Kawato, M. "A framework for learning biped locomotion with dynamical movement primitives." In "2004 4th IEEE/RAS International Conference on Humanoid Robots," Vol. 2, pp. 925–940, Nov 2004.
8. El-Sayed, A.M., Hamzaid, N.A. and Osman, N.A.A. "Technology efficacy in active prosthetic knees for transfemoral amputees: A quantitative evaluation." *The Scientific World Journal*, p. 17, 2014.
9. Nakamura, M., Goto, S. and Kyura, N. *Mechatronics servo system control*. Springer, 1998.
10. Kehua, M., Xiao, M. and Lincen, Z. "Adaptive control of biped robots based on gennet." In "Computer Science Education (ICCSE), 2012 7th International Conference on," pp. 1018–1020, July 2012.
11. Istepanian, R. and Whidborne, J. *Digital Controller Implementation and Fragility.* Springer, 2001.
12. Schaal, S., Ijspeert, A., Billard, A., Vijayakumar, S. and Meyer, J. *GasNets and other Evolvable Neural Networks applied to Bipedal Locomotion*. MIT Press, 2004.
13. Bartolini, G., Fridman, L., Pisano, A. and Usai, E. *Modern Sliding Mode Control Theory New Perspectives and Applications*. Springer, 2008.
14. Spong, M.W., Hutchinson, S. and Vidyasagar, M. *Robot Modeling and Control*. 1 ed.. Wiley, 2006.
15. Reyes, F. and Kelly, R. "Experimental evaluation of identification schemes on a direct drive robot." *Robotica*, Vol. 15, No. 05, pp. 563–571, 1997.
16. Clarke, D.W., Mohtadi, C. and Tuffs, P. "Generalized predictive control, part i the basic algorithm." *Automatica*, Vol. 23, pp. 137–148, 1987.
17. Garcia, C.E., Prett, D.M. and Morari, M. "Model predictive control: Theory and practice: A survey." *Automa*, Vol. 25, pp. 335–348, 1989.
18. Camacho, E.F. and Bordons Alba, C. *Model Predictive Control*. Springer, 2007.
19. Rossiter, J.A. *Model Based Predictive control*. CRC press, 2003.
20. Awrynzuk, M. "On improving accuracy of computationally efficient nonlinear predictive control based on neural models." *Chemical Engineering Science*, Vol. 66, pp. 5253–5267, 2011.
21. Zhang, Y. *Model Predictive Cascade Control*. Master's thesis, School of Electrical & Electronic Eng., 2003.